Syntheses and Characterization of Dinuclear Manganese(II,II) and Manganese(II,III) Complexes with Phenolate and Two Carboxylate Bridges

Masatatsu SUZUKI, Masahiro MIKURIYA,† Shuji MURATA, Akira UEHARA,* Hiroki OSHIO,† Sigeo KIDA,† and Kazuo SAITO†

Department of Chemistry, Faculty of Science, Kanazawa University, Kanazawa 920
†Coordination Chemistry Laboratories, Institute for Molecular Science, Okazaki 444

(Received May 27, 1987)

Dinuclear manganese(II,II) and (II,III) complexes, $[Mn_2(L\text{-}py)(RCOO)_2]ClO_4 \cdot nH_2O$ and $[Mn_2(L\text{-}py)(RCOO)_2](ClO_4)_2 \cdot nH_2O$, were prepared, where L-py is 2,6-bis[bis(2-pyridylmethyl)aminomethyl]-4-methylphenolate(1−) and RCOO denotes CH_3COO or C_6H_5COO. X-Ray structure analysis of the mixed valence complex $[Mn_2(L\text{-}py)(C_6H_5COO)_2](ClO_4)_2 \cdot H_2O$ revealed that the complex cation involves octahedral manganese(II) and manganese(III) centers with N_3O_3 donor sets and that the two metal ions are linked by phenolato and two benzoato groups. Magnetic susceptibility measurements over temperature range 80—300 K indicated that both manganese(II,II) and (II,III) complexes exhibit weak antiferromagnetic interaction with spin-exchange coupling constant, $J=-5$—-7 cm^{-1}. Cyclic voltammograms of the mixed valence complexes showed two quasi-reversible redox couples at ca. 0.5 and ca. 1.0 V (vs. SCE), assignable to the redox reactions of Mn^{II}-Mn^{III}/Mn^{II}-Mn^{II} and Mn^{III}-Mn^{III}/Mn^{II}-Mn^{III}, respectively. The comproportionation constants for the reaction $(Mn^{III}\text{-}Mn^{III})+(Mn^{II}\text{-}Mn^{II}) \rightleftarrows 2(Mn^{II}\text{-}Mn^{III})$ at 20 °C were estimated as $2\text{—}3\times10^9$.

It has been pointed out that the manganese ions in the water oxidizing system of photosystem II in green plants are present as dinuclear or tetranulclear cluster, in which the di-, tri-, and/or tetravalent manganese ions are involved in the catalytic cycle of water oxidation.[1,2] Although many efforts have been devoted to understanding the role of the manganese ions operating in the cycle, little is known on the structure of the manganese site and the reaction mechanism of water oxidation.

It has been suggested that a mixed valence dinuclear manganese(II,III) center exists in chloroplasts in the dark.[3,4] For further elucidation of the above manganese site, it is needed to study in more detail the coordination chemistry of dinuclear mixed valence manganese(II,III) complexes with biologically relevant ligands such as 2- or 4-imidazolyl group, carboxylato and phenolato groups, etc. However, only a few suitable model complexes have been devised for this purpose.[5,6]

In the previous paper, we shortly communicated the synthesis and characterization of a mixed valence manganese(II, III) complex $[Mn_2(L\text{-}py)(CH_3COO)_2](ClO_4)_2 \cdot H_2O$, and proposed a dinuclear structure in which manganese(II) and manganese(III) ions are bridged by the phenolato and two acetato groups.[7] Reported herein are syntheses and the physicochemial properties of the dinuclear manganese(II, II) and (II, III) complexes with a dinucleating ligand (L-py) and a carboxylate ion, $[Mn_2(L\text{-}py)(RCOO)_2]ClO_4 \cdot nH_2O$ and $[Mn_2(L\text{-}py)(RCOO)_2](ClO_4)_2 \cdot nH_2O$ ($RCOO=CH_3COO$ or C_6H_5COO), where L-py represents 2,6-bis[bis(2-pyridylmethyl)aminomethyl]-4-methylphenolate(1−) ion. The crystal structure of $[Mn_2(L\text{-}py)(C_6H_5COO)_2](ClO_4)_2 \cdot H_2O$ is also described, which is the first example of a mixed valence manganese(II, III) complex whose structure was determined by X-ray structure analysis.

Experimental

Materials. HL-py was synthesized as previously described.[8] $[Mn(dmso)_6](ClO_4)_3$ was prepared according to the method of literature.[9] The other chemicals were of reagent grade.

Preparation of Manganese(II, II) Complexes. $[Mn_2(L\text{-}py)(CH_3COO)_2]ClO_4 \cdot 0.5H_2O$ (**1a**): A solution of $Mn(CH_3COO)_2 \cdot 4H_2O$ (1 mmol) in 20 cm^3 of methanol was added with stirring to a solution of HL-py (0.5 mmol), triethylamine (1 mmol), and $NaClO_4$ (2 mmol) in 20 cm^3 of methanol. White crystals formed were filtered off, washed with ethanol and ether, and dried in vacuo.

$[Mn_2(L\text{-}py)(C_6H_5COO)_2]ClO_4 \cdot 2H_2O$ (**2a**): A solution of $Mn(ClO_4)_2 \cdot 6H_2O$ (1 mmol) in 20 cm^3 of methanol was added to a methanol solution (20 cm^3) of HL-py (0.5 mmol), C_6H_5COOH (1 mmol), and triethylamine (1.5 mmol) with stirring. White crystals obtained were filtered off, washed with ethanol and ether, and dried in vacuo.

Preparation of Manganese(II, III) Complexes. $[Mn_2(L\text{-}py)(CH_3COO)_2](ClO_4)_2 \cdot H_2O$ (**1b**): A solution of $Mn(CH_3COO)_3 \cdot 2H_2O$ (1 mmol) in 30 cm^3 of methanol was mixed with a solution of HL-py (0.5 mmol) in 20 cm^3 of methanol with stirring. To the resulting solution was added a methanol solution (20 cm^3) of $NaClO_4$ (4 mmol) to give dark green crystals, which were filtered off, washed with ethanol and ether, and dried in vacuo. Recrystallization was carried out from acetonitrile.

$[Mn_2(L\text{-}py)(C_6H_5COO)_2](ClO_4)_2 \cdot H_2O$ (**2b**): A solution of HL-py (0.5 mmol), C_6H_5COOH (1 mmol), and triethylamine (1.5 mmol) in 20 cm^3 of methanol was added to a suspension of $[Mn(dmso)_6](ClO_4)_3$ (1 mmol) in 30 cm^3 of acetone with stirring. The mixture was strirred for 30 min and filtered to remove the unreacted dmso complex. The filtrate was allowed to stand overnight to produce dark green crystals. They were recrystallized from acetonitrile.

Measurements. The electronic spectra in acetonitrile solution were measured on a Jasco UVIDEC 505 UV/VIS recording digital spectrophotometer and a Hitachi 323 recording spectrophotometer.

Infrared spectra were obtained by a KBr-disk method and a nujol mull method with a Jasco A-3 infrared spectrophotometer.

Magnetic susceptibilities were measured with a Shimazu torsion magnetometer MB-2 which was calibrated with $Hg[Co(NCS)_4]$. Diamagnetic correction was made by using Pascal's constants.

Cyclic voltammograms were obtained with a Yanagimoto P-900 in a cell containing a glassy carbon working electrode, a platinum-coil auxiliary electrode, and a saturated calomel electrode as reference electrode. Applied voltage was measured with a Takeda Riken TR-8651 electrometer. Acetonitrile was used as the solvent and tetrabutylammonium perchlorate as the supporting electrolyte. Ferrocene was added for an internal check on redox potential and reversibility. $E_{1/2}$ of ferrocene was 0.39 V (vs. SCE) with a peak-to-peak separation (ΔE) of 70 mV. For constant-potential electrolyses, Hokuto Denko HA-301 potentiostat/galvanostat was used to control the potentials. Current-time curves were recorded with a Rikenn Denshi SP-K1V recorder. Integration of current was carried out by integrating the area under the current vs. time curves. A two compartmental H-type cell with a glass frit containing a platinum gauze working electrode, platinum plate auxiliary electrode, and a saturated caromel electrode was used. For the reduction and oxidation of **1b**, applied potentials were +0.35 and +1.15 V (vs. SCE), respectively.

ESR spectra were measured on a JEOL JES-FE2XG ESR spectrometer (X-band microwave unit, 100 KHz field modulation) equipped with an Air Product LTD-3-110 liquid helium transfer system. The microwave frequency was monitored with a Takeda Riken TR5212 microwave counter, and the resonance magnetic field values of the signals were measured with an NMR field meter (ECHO Electronics Co., Ltd.)

Analyses of Manganese(II) and Manganese(III) Ions. Analysis of manganese(III) ion was carried out by iodometry and by the method described in the literature.[10] Total amount of manganese ion was determined colorimetrically.[11] The results are listed in Table 1.

X-Ray Crystal Structure Analysis of $[Mn_2(L\text{-}py)(C_6H_5COO)_2](ClO_4)_2\cdot H_2O$. Crystal data: $[Mn_2(C_{33}H_{33}N_6O)(C_6H_5COO)_2](ClO_4)_2\cdot H_2O$; $F.W.$=1098.69, monoclinic; $P2_1/c$; a=23.979 (4), b=11.357(1), and c=18.502(2) Å; β=97.29(1)°; V=4997.8(12) Å^3; Graphite monochromated Mo$K\alpha$ (λ=0.71073 Å); D_m=1.50, D_c=1.46 g cm^{-3}; Z=4; μ (Mo$K\alpha$)=6.60 cm^{-1}; A dark green crystal with dimensions of 0.10×0.18×0.37 mm.

Data Collection and Processing: The unit-cell parameters and intensities were measured on a Rigaku AFC-5 automated four-circle diffractometer by the 2θ-ω scan technique with a scan rate of 3° min^{-1}. A total of 9543 reflections with $2\theta < 50°$ was collected. Three standard reflections were monitored every 50 reflections. The intensities of two standard reflections showed a good stability, although one reflection underwent a significant decay: the intensities decreased to ca. 35% of initial intensity at the end of measurement. All attempts to obtain better single crystals were in vain, because the crystals were very fragile and not suitable for measurement. Therefore we used the above intensity data for analysis without correction for the intensity decay. The intensity data were corrected for the Lorentz-polarization effects and for absorption. Independent 3590 reflections with $|F_o| > 3\sigma(|F_o|)$ were considered as "observed" and were used for the structure analysis.

The structure was solved by the direct method. Refinement was carried out by the block-diagonal least-squares method. Oxygen atom of water molecule was found to be statistically distributed at two positions with occupancy factor of 0.5. All the non-hydrogen atoms were refined with isotropic thermal parameters. Hydrogen atoms were not included in the calculation. The weighting scheme $w=[\sigma^2_{count}+(0.015|F_o|)^2]^{-1}$ was employed. The final discrepancy factors were $R=\sum||F_o|-|F_c||/\sum|F_o|=0.116$ and $R_w=[\sum w(|F_o|-|F_c|)^2/\sum w|F_o|^2]^{1/2}=0.118$.

The atomic scattering factors and the anomalous dispersion corrections, $\Delta f'$ and $\Delta f''$, for Mn, Cl, O, N, and C, were taken from the International Tables for X-Ray Crystallography.[12] All the calculations were carried out on the HITAC M-680H computer at the Computer Center of the Institute for Molecular Science by the use of the UNICS-III,[13] MULTAN 78,[14] and ORTEP[15] programs. The final positional and thermal parameters of non-hydrogen atoms with their estimated standard deviations are given in Table 2. Observed and Calculated structure factors have been deposited as a Document No. 8773 at the office of the Editor.

Results and Discussion

Structure Description of $[Mn_2(L\text{-}py)(C_6H_5COO)_2](ClO_4)_2\cdot H_2O$. Figure 1 shows a perspective view of the complex cation and the numbering system of

Table 1. Analytical Data and Effective Magnetic Moments of the Complexes

	Complex	Found (Calcd) (%)					μ_{eff} (Mn_2)/ B.M.[a]
		C	H	N	Mn(II)	Mn(III)	
1a	$[Mn_2(L\text{-}py)(CH_3COO)_2]ClO_4\cdot 0.5H_2O$	51.30 (51.31)	4.34 (4.66)	9.33 (9.70)			7.8
2a	$[Mn_2(L\text{-}py)(C_6H_5COO)_2]ClO_4\cdot 2H_2O$	54.80 (55.49)	4.23 (4.66)	8.20 (8.26)			7.7
1b	$[Mn_2(L\text{-}py)(CH_3COO)_2](ClO_4)_2\cdot H_2O$	45.47 (45.60)	3.90 (4.23)	8.31 (8.62)	5.2 (5.64)	5.6 (5.64)	7.1
2b	$[Mn_2(L\text{-}py)(C_6H_5COO)_2](ClO_4)_2\cdot H_2O$	51.26 (51.38)	3.79 (4.13)	7.73 (7.65)	5.0 (5.00)	5.0 (5.00)	7.1

a) At room temperature.

Table 2. Fractional Positional Parameters ($\times 10^4$) and Thermal Parameters of Non-Hydrogen Atoms with Their Estimated Standard Deviations in Parentheses

Atom	x	y	z	B/Å^3	Atom	x	y	z	B/Å^3
Mn(1)	2814(1)	−1794(2)	1662(1)	2.9(0.1)	C(12)	4290(8)	−4499(18)	1322(10)	6.0(0.5)
Mn(2)	1925(1)	446(2)	929(1)	3.0(0.1)	C(13)	3746(8)	−4813(18)	1062(10)	5.8(0.5)
Cl(1)	5543(2)	−2896(5)	3232(3)	5.7(0.1)	C(14)	3298(7)	−4051(15)	1152(9)	4.4(0.4)
Cl(2)	461(3)	6158(6)	2379(3)	8.2(0.2)	C(15)	3537(6)	−2025(15)	3125(8)	3.5(0.4)
O(1)	2375(4)	−465(9)	1866(5)	3.0(0.2)	C(16)	2968(6)	−2443(14)	3237(8)	3.4(0.4)
O(2)	3131(4)	−877(9)	785(5)	3.8(0.2)	C(17)	2847(7)	−2662(16)	3957(9)	5.0(0.5)
O(3)	2599(4)	587(9)	294(5)	3.9(0.2)	C(18)	2323(8)	−3154(18)	4037(10)	6.1(0.5)
O(4)	2230(4)	−2716(9)	1095(5)	3.6(0.2)	C(19)	1927(7)	−3428(16)	3427(9)	5.2(0.5)
O(5)	1648(4)	1293(10)	568(5)	4.1(0.3)	C(20)	2079(7)	−3120(15)	2730(8)	3.9(0.4)
OP(1)	5072(6)	−2191(14)	3381(8)	8.5(0.4)	C(21)	1327(7)	−67(15)	2346(8)	3.7(0.4)
OP(2)	5719(7)	−2551(15)	2564(9)	10.5(0.5)	C(22)	1231(6)	2035(15)	1907(8)	3.6(0.4)
OP(3)	5998(6)	−2773(14)	3784(8)	9.1(0.4)	C(23)	1799(6)	2565(14)	1962(6)	3.1(0.3)
OP(4)	5376(7)	−4065(16)	3178(9)	11.4(0.5)	C(24)	1961(7)	3485(15)	2462(9)	4.6(0.4)
OP(5)	751(7)	7027(15)	2025(9)	10.5(0.5)	C(25)	2497(8)	3944(17)	2504(10)	5.3(0.5)
OP(6)	498(8)	6406(18)	3154(10)	13.8(0.6)	C(26)	2858(8)	3491(17)	2060(9)	5.2(0.5)
OP(7)	−107(7)	6018(15)	2075(8)	10.0(0.5)	C(27)	2677(7)	2596(15)	1566(9)	4.0(0.4)
OP(8)	728(10)	5119(21)	2302(12)	16.5(0.8)	C(28)	704(7)	412(15)	1225(8)	4.1(0.4)
OW	4761(10)	2013(22)	4828(12)	5.7(0.6)[a]	C(29)	697(7)	1000(15)	476(9)	4.0(0.4)
OW′	4406(10)	604(22)	4476(12)	5.9(0.6)[a]	C(30)	186(7)	1410(16)	123(9)	5.0(0.4)
N(1)	3489(5)	−1261(11)	2437(6)	3.6(0.3)	C(31)	188(8)	1913(17)	−559(10)	5.4(0.5)
N(2)	3414(5)	−2978(12)	1494(7)	4.0(0.3)	C(32)	677(8)	1900(18)	−901(10)	5.9(0.5)
N(3)	2597(5)	−2655(11)	2665(6)	3.2(0.3)	C(33)	1161(7)	1466(16)	−482(9)	4.9(0.4)
N(4)	1245(5)	741(11)	1685(6)	3.1(0.3)	C(34)	3023(6)	−45(14)	339(8)	3.1(0.3)
N(5)	2158(5)	2154(11)	1533(6)	3.0(0.3)	C(35)	3441(6)	153(14)	−193(8)	3.1(0.3)
N(6)	1172(5)	1034(11)	191(6)	3.4(0.3)	C(36)	3925(7)	−556(15)	−171(9)	4.3(0.4)
C(1)	2383(6)	−20(14)	2551(8)	2.7(0.3)	C(37)	4293(7)	−411(16)	−693(9)	4.8(0.4)
C(2)	2893(6)	223(14)	2941(8)	3.2(0.3)	C(38)	4177(7)	467(16)	−1220(9)	4.9(0.4)
C(3)	2917(7)	653(15)	3669(9)	4.3(0.4)	C(39)	3713(8)	1201(17)	−1245(9)	5.2(0.5)
C(4)	2393(7)	820(15)	3942(8)	3.9(0.4)	C(40)	3326(7)	1056(15)	−705(9)	4.2(0.4)
C(5)	1882(7)	626(15)	3527(8)	4.1(0.4)	C(41)	1783(6)	−2351(14)	688(8)	3.6(0.4)
C(6)	1887(6)	190(14)	2814(8)	3.4(0.4)	C(42)	1391(6)	−3299(14)	330(8)	3.4(0.3)
C(7)	2406(7)	1260(16)	4772(9)	4.7(0.4)	C(43)	1370(7)	−4407(16)	635(9)	4.7(0.4)
C(8)	3431(7)	37(14)	2622(8)	3.6(0.4)	C(44)	975(8)	−5270(18)	304(10)	5.9(0.5)
C(9)	4003(6)	−1452(14)	2079(8)	3.4(0.4)	C(45)	662(8)	−4944(19)	−362(11)	6.7(0.5)
C(10)	3944(7)	−2653(15)	1742(8)	3.8(0.4)	C(46)	691(8)	−3851(16)	−687(9)	4.9(0.4)
C(11)	4413(8)	−3387(17)	1657(10)	5.5(0.5)	C(47)	1057(6)	−2974(15)	−323(8)	3.7(0.4)

a) Ocuppancy factor of 0.5.

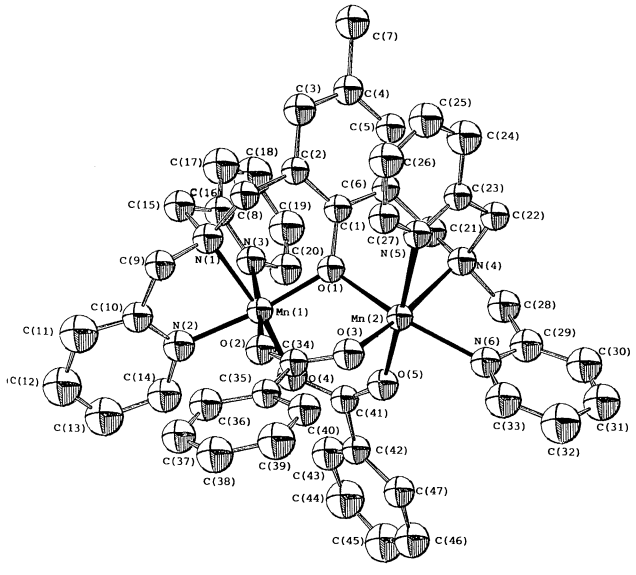

Fig. 1. Crystal structure of the complex cation $[Mn_2(L\text{-}py)(C_6H_5COO)_2]^{2+}$ showing the 50% probability thermal ellipsoids and the atom-labeling scheme.

atoms. The selected bond distances and anlges are listed in Table 3. The crystal structure consists of a discrete dinuclear cation $[Mn_2(L\text{-}py)(C_6H_5COO)_2]^{2+}$, two perchlorate anions, and a water molecule which is statistically distributed to the two positions. Each manganese atom is in a distorted octahedral coordination with a cis,cis-N_3O_3 configuration. The bond distances around the Mn(1) and Mn(2) moieties significantly differ from each other. The bond distances of Mn(1)-O and Mn(1)-N are in the ranges of 1.905(10)—2.147(11) Å and 2.022(14)—2.217(12) Å, respectively, while those of Mn(2)-O and Mn(2)-N are in the ranges of 2.123(11)—2.184(9) Å and 2.224(12)—2.304(13) Å, respectively. The Mn(1)-O and Mn(1)-N distances are comparable to those reported for manganese(III) complexes[16,17] and the Mn(2)-O and Mn(2)-N ones to those reported for manganese(II) complexes.[18] In the Mn(1) moiety, the Mn(1)-O(2) and Mn(1)-N(3) distances are much longer than Mn(1)-O(1), Mn(1)-O(4), Mn(1)-N(1), and Mn(1)-N(2) ones. The O(1), O(4), N(1), and N(2) atoms form an approximate square

Table 3. Selected Interatomic Distances (l/Å) and Angles (ϕ/°) of $[Mn_2(L\text{-py})(C_6H_5COO)_2](ClO_4)_2 \cdot H_2O$

(a) Manganese coordination spheres				(c) L-py moiety			
Mn(1)-Mn(2)	3.483(3)			O(1)-C(1)	1.363(17)		
(Mn(1) moiety)		(Mn(2) moiety)		(Mn(1) moiety)		(Mn(2) moiety)	
Mn(1)-O(1)	1.905(10)	Mn(2)-O(1)	2.184(9)	N(1)-C(8)	1.524(21)	N(4)-C(21)	1.521(20)
Mn(1)-O(2)	2.147(11)	Mn(2)-O(3)	2.123(11)	N(1)-C(9)	1.489(21)	N(4)-C(22)	1.527(21)
Mn(1)-O(4)	1.947(10)	Mn(2)-O(5)	2.162(11)	N(1)-C(15)	1.533(20)	N(4)-C(28)	1.504(19)
Mn(1)-N(1)	2.110(12)	Mn(2)-N(4)	2.304(13)	N(2)-C(10)	1.348(20)	N(5)-C(23)	1.327(20)
Mn(1)-N(2)	2.022(14)	Mn(2)-N(5)	2.273(12)	N(2)-C(14)	1.385(22)	N(5)-C(27)	1.335(20)
Mn(1)-N(3)	2.217(12)	Mn(2)-N(6)	2.224(12)	N(3)-C(16)	1.315(18)	N(6)-C(29)	1.316(21)
				N(3)-C(20)	1.370(20)	N(6)-C(33)	1.334(21)
Mn(1)-O(1)-Mn(2)	116.6(5)			C(1)-C(2)	1.367(20)	C(2)-C(3)	1.426(22)
O(1)-Mn(1)-O(2)	91.3(4)	O(1)-Mn(2)-O(3)	98.1(4)	C(2)-C(8)	1.501(23)	C(6)-C(21)	1.532(21)
O(1)-Mn(1)-O(4)	98.9(4)	O(1)-Mn(2)-O(5)	85.1(4)	C(9)-C(10)	1.499(23)	C(22)-C(23)	1.481(22)
O(1)-Mn(1)-N(1)	91.9(5)	O(1)-Mn(2)-N(4)	84.5(4)	C(15)-C(16)	1.484(22)	C(28)-C(29)	1.535(23)
O(1)-Mn(1)-N(2)	168.3(5)	O(1)-Mn(2)-N(5)	87.0(4)	Mn(1)-O(1)-C(1)	122.4(8)	Mn(2)-O(1)-C(1)	120.6(9)
O(1)-Mn(1)-N(3)	89.4(4)	O(1)-Mn(2)-N(6)	155.7(4)	Mn(1)-N(1)-C(8)	110.2(9)	Mn(2)-N(4)-C(21)	111.7(9)
O(2)-Mn(1)-O(4)	98.8(4)	O(3)-Mn(2)-O(5)	97.1(4)	Mn(1)-N(1)-C(9)	105.2(8)	Mn(2)-N(4)-C(22)	110.1(9)
O(2)-Mn(1)-N(1)	93.5(4)	O(3)-Mn(2)-N(4)	166.7(4)	Mn(1)-N(1)-C(15)	111.9(9)	Mn(2)-N(4)-C(28)	104.2(9)
O(2)-Mn(1)-N(2)	83.1(5)	O(3)-Mn(2)-N(5)	92.9(4)	Mn(1)-N(2)-C(10)	115.1(11)	Mn(2)-N(5)-C(23)	117.1(10)
O(2)-Mn(1)-N(3)	171.9(4)	O(3)-Mn(2)-N(6)	104.7(4)	Mn(1)-N(2)-C(14)	123.4(10)	Mn(2)-N(5)-C(27)	120.9(10)
O(4)-Mn(1)-N(1)	163.4(5)	O(5)-Mn(2)-N(4)	96.2(4)	Mn(1)-N(3)-C(16)	112.7(10)	Mn(2)-N(6)-C(29)	114.9(10)
O(4)-Mn(1)-N(2)	92.1(5)	O(5)-Mn(2)-N(5)	168.0(4)	Mn(1)-N(3)-C(20)	123.8(9)	Mn(2)-N(6)-C(33)	127.0(11)
O(4)-Mn(1)-N(3)	89.1(4)	O(5)-Mn(2)-N(6)	83.7(4)	C(20)-N(3)-C(16)	121.9(13)	C(33)-N(6)-C(29)	118.1(13)
N(1)-Mn(1)-N(2)	78.3(5)	N(4)-Mn(2)-N(5)	74.1(4)	O(1)-C(1)-C(2)	118.1(13)	O(1)-C(1)-C(6)	119.3(12)
N(1)-Mn(1)-N(3)	78.4(5)	N(4)-Mn(2)-N(6)	75.4(4)	C(2)-C(1)-C(6)	122.7(14)	C(1)-C(2)-C(3)	119.6(15)
N(2)-Mn(1)-N(3)	94.8(5)	N(5)-Mn(2)-N(6)	100.1(4)	C(1)-C(2)-C(8)	121.4(13)	C(1)-C(6)-C(21)	120.5(13)
				N(1)-C(8)-C(2)	109.4(13)	N(4)-C(21)-C(6)	110.8(13)
(b) Benzoate moiety				N(1)-C(9)-C(10)	106.1(13)	N(4)-C(22)-C(23)	111.1(13)
O(2)-C(34)	1.260(18)	O(4)-C(41)	1.297(17)	N(2)-C(10)-C(9)	115.3(14)	N(5)-C(23)-C(22)	118.5(13)
O(3)-C(34)	1.240(18)	O(5)-C(41)	1.258(20)	N(1)-C(15)-C(16)	108.8(12)	N(4)-C(28)-C(29)	108.3(13)
O(34)-C(35)	1.506(22)	O(41)-C(42)	1.525(22)	N(3)-C(16)-C(15)	119.1(13)	N(6)-C(29)-C(28)	117.6(13)
Mn(1)-O(2)-C(34)	142.9(10)	Mn(2)-O(3)-C(34)	126.6(10)				
Mn(1)-O(4)-C(41)	128.8(10)	Mn(2)-O(5)-C(41)	139.1(9)				
O(2)-C(34)-O(3)	125.1(14)	O(4)-C(41)-O(5)	125.8(14)				
O(2)-C(34)-O(35)	116.3(13)	O(4)-C(41)-C(42)	116.5(14)				
O(3)-C(34)-C(35)	118.5(13)	O(5)-C(41)-C(42)	117.8(13)				

plane involving Mn(1) atom at its center. The coordination geometry around Mn(1) is best described as an elongated octahedron, which is attributable to the Jahn-Teller effect of high spin d^4 ion (vide infra). Thus, the molecular structure clearly shows that the present complex consists of manganese(II) and manganese(III) ions whose valence states are firmly trapped.

The intramolecular Mn(1)-Mn(2) distance is 3.484 (3) Å. The manganese atoms are triply bridged by phenolate oxygen and two benzoate oxygens to form a cofacial bioctahedral structure. Such triply bridging structures have been found for some dinuclear manganese and iron complexes with bridging groups composed of two carboxylate and one oxide (hydroxide, or phenolate) ions.[19-22]

Two benzoato groups bridge the manganese atoms in syn-syn configuration. However, the bridging benzoato groups are not equivalent: one symmetrically bridges the manganese atoms, whereas the other does unsymmetrically. The Mn(1)-O(2) (2.147(11) Å) and Mn(2)-O(3) (2.123(11) Å) bonds of symmetrically bridging benzoato group are close to each other in length. However, the Mn(1)-O(4) (1.947(10) Å) and Mn(2)-O(5) (2.162(11) Å) bond lengths of unsymmetrically bridging benzoato group significantly differ from each other.

IR Spectra. The infrared spectrum of **2b** shows one $\nu_{asymm}(COO^-)$ at 1567 cm^{-1} and two $\nu_{symm}(COO^-)$ at 1407 and 1370 cm^{-1} (Fig. 2), indicating the presence of two types of benzoato groups, which is compatible with the result of X-ray structural analysis mentioned above. The $\Delta\nu$ value ($\nu_{asymm}(COO^-)-\nu_{symm}(COO^-)$) is useful for the diagnosis of coordination mode of carboxylato group, i.e., a symmetrically bridging carboxylato group gives $\Delta\nu$ value smaller than 200 cm^{-1}, whereas an unsymmetrically bridging one and monodentate one larger $\Delta\nu$ values.[23] Thus, the larger $\Delta\nu$ (197 cm^{-1}) of **2b** is assigned to that of the unsymmetrically bridging carboxylato group and the smaller value (160 cm^{-1}) to that of the symmetrically bridging one. On the other hand, the dinuclear manganese(II, II) complex **2a** shows one $\nu_{asymm}(COO^-)$ and one $\nu_{symm}(COO^-)$ at 1570 and 1400 cm^{-1} ($\Delta\nu$=170 cm^{-1}), respectively, indicating that the two carboxylato groups are equivalent and symmetrically bridge two manganese(II) ions. The complex **2a** seems to have a triply bridging structure similar to that of **2b**.

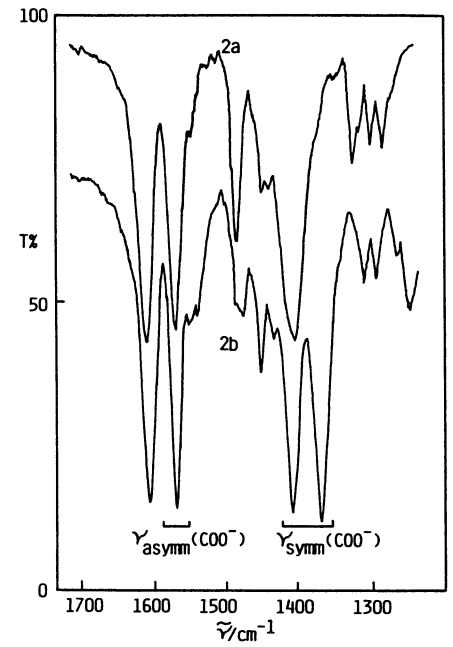

Fig. 2. Infrared spectra of $[Mn_2(L\text{-}py)(C_6H_5COO)_2]ClO_4\cdot 2H_2O$ (**2a**) and $[Mn_2(L\text{-}py)(C_6H_5COO)_2](ClO_4)_2\cdot H_2O$ (**2b**).

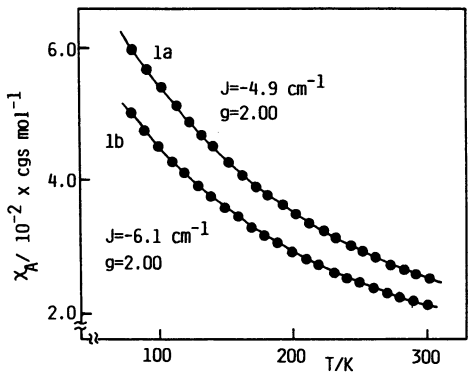

Fig. 3. Temperature dependence of magnetic susceptibilities of $[Mn_2(L\text{-}py)(CH_3COO)_2]ClO_4\cdot 0.5H_2O$ (**1a**) and $[Mn_2(L\text{-}py)(CH_3COO)_2](ClO_4)_2\cdot H_2O$ (**1b**).

Magnetic Susceptibilities. The effective magnetic moments of **1a** and **2a** at room temperature are 7.8 and 7.7 B.M./Mn_2, and those of **1b** and **2b** are 7.1 and 7.1 B.M./Mn_2, respectively, indicating that all the manganese(II) and (III) ions in the above complexes are of high spin. Magnetic susceptibilities of the complexes were measured in the temperature range from 80 to 300 K. The results were analyzed by the usual spin-spin interaction model based on exchange Hamiltonian $H=-2JS_1\cdot S_2$. The molar magnetic susceptibility of (χ_A) of an $S_1=5/2\cdot S_2=5/2$ spin exchange coupling dimer is given in Eq. 1, and that of an $S_1=2\cdot S_2=5/2$ spin exchange coupling dimer by Eq. 2,

$$\chi_A=\frac{2N\beta^2g^2}{\kappa T}\cdot\frac{x^{28}+5x^{24}+14x^{18}+30x^{10}+55}{x^{30}+3x^{28}+5x^{24}+7x^{18}+9x^{10}+11}+N\alpha \quad (1)$$

$$\chi_A=\frac{N\beta^2g^2}{4\kappa T}\cdot\frac{x^{24}+10x^{21}+35x^{16}+84x^{9}+165}{x^{24}+2x^{21}+3x^{16}+4x^{9}+5}+N\alpha \quad (2)$$

where $x=\exp(-J/\kappa T)$ and the symbols have their usual meanings. Figure 3 shows temperature dependence of the magnetic susceptibilities of **1a** and **1b**. The solid lines are the calculated curves by using the paremeters listed in Table 4. Both dinuclear manganese(II, II) and (II, III) complexes exhibit weak antiferromagnetic interaction (J=−4.9—−6.3 cm^{-1}: Table 4). The corresponding dinuclear mixed valence iron(II, III) complexes $[Fe_2(L\text{-}py)(RCOO)_2](BF_4)_2\cdot nH_2O$ and $[Fe_2(L\text{-}py)(CH_3COO)(OH)](BF_4)_2\cdot 2H_2O$ exhibited comparable magnitude of antiferromagnetic interaction (J=−3—−8 cm^{-1}).[24] These results suggest that the triply bridging unit consisting of phenolate and two carboxylate ions provides an weak antiferromagnetic interaction, regardless of the species (Fe or Mn ion) and oxidation state of metal ion.

Electronic Spectra. The aborption spectra of **1a** and **1b** are shown in Fig. 4. The complex **1a** shows no appreciable absorption in the region below 25000

Table 4. Magnetic Parameters of the Complexes

	Complex	J/cm^{-1}	g	Nα/10^{-6} cgs mol^{-1}
1a	$[Mn_2(L\text{-}py)(CH_3COO)_2]ClO_4\cdot 0.5H_2O$	−4.9	2.00	0
2a	$[Mn_2(L\text{-}py)(C_6H_5COO)_2]ClO_4\cdot 2H_2O$	−5.5	2.00	0
1b	$[Mn_2(L\text{-}py)(CH_3COO)_2](ClO_4)_2\cdot H_2O$	−6.1	2.00	0
2b	$[Mn_2(L\text{-}py)(C_6H_5COO)_2](ClO_4)_2\cdot H_2O$	−6.3	2.00	0

Table 5. Electronic Spectral Data of the Mixed Valence Complexes in Acetonitrile

	Complex	$\tilde{\nu}_{max}$ 10^3×cm^{-1}, (ε/mol^{-1} dm^3 cm^{-1})		
1b	$[Mn_2(L\text{-}py)(CH_3COO)_2](ClO_4)_2\cdot H_2O$	16.2(870)	17.8(820)	20.9(1230)
		21.7(1220)	23.4(1280)^s	26.0(1560)
2b	$[Mn_2(L\text{-}py)(C_6H_5COO)_2](ClO_4)_2\cdot H_2O$	15.8(830)	17.8(760)	20.8(1170)^s
		21.6(1180)^s	23.4(1290)^s	25.9(1490)

s: Shoulder.

cm^{-1}, indicating the electronic configuration of manganese(II) ion to be of high spin. The mixed valence complex **1b** exhibits six absorption bands including shoulders in the visible and near ultraviolet regions (Fig. 4 and Table 5). In general, six-coordinated manganese(III) complex displays one or two d-d bands (^5E_g to $^5T_{2g}$ electronic transitions in octahedral symmetry) in these regions.[17,25] The molar extinction coefficients of **1b** and **2b** are 800—1500 mol^{-1} dm^3cm^{-1}, which are considerably larger than those of d-d transitions of manganese(III) complexes. Judging from the numbers of absorption bands and their intensities, all the six bands can not be ascribed to the d-d transitions. Charge transfer transitions from $p\pi$ orbital of bridging phenolato group to half filled $d\pi^*$ orbitals of manganese(III) ion may appear in these regions as was observed for iron(III)-phenolato complexes.[26] It is also possible that intervalence charge transfer transition(IT) from Mn^{II} moiety to Mn^{III} moiety appears in these regions. More detailed assignment is not possible at the present stage.

It should be noted that the present mixed valence complexes exhibit no IT bands in the near infrared region, whereas the iron complexes $[Fe_2(L)(RCOO)_2]^{2+}$ (L=L-py or L-Bzim) (L-Bzim=2,6-bis[bis(2-benzimidazolylmethyl)aminomethyl]-4-methylphenolate(1−) ion) showed an intense IT band at that region.[24,27] This fact might be due to a smaller extent of electron delocalization in the manganese complexes than that in the iron complexes.

Cyclic Voltammogram. Figure 5 illustrates the cyclic voltammogram of **1b** in acetonitrile at 20 °C. This complex shows two quasi-reversible redox couples at +1.02 and +0.47 V (vs. SCE). Controlled potential electrolysis of the complex **1b** was carried out in order to determine the number of electrons (n) transferred in the above two processes. The oxidation of the complex at +1.15 V and reduction at +0.35 V (vs. SCE) gave n values of 1.1±0.1 and 0.9±0.1, respectively, indicating that those two redox couples correspond to one-electron redox reactions assignable to $E_{1/2}{}^a$ (Mn^{III}-Mn^{III}/Mn^{II}-Mn^{III} (+1.02 V)) and $E_{1/2}{}^b$ (Mn^{II}-Mn^{III}/Mn^{II}-Mn^{II} (+0.47 V)). The complex **2b** also showed a similar cyclic voltammogram (Table 6).

From the separation of the redox potentials, $E_{1/2}{}^a$ and $E_{1/2}{}^b$, comproportionation constant (K at 20 °C) of the following reaction can be calculated by Eq. 3.

$$(Mn^{III}\text{-}Mn^{III})+(Mn^{II}\text{-}Mn^{II}) \rightleftarrows 2(Mn^{III}\text{-}Mn^{II})$$
$$E_{1/2}{}^a - E_{1/2}{}^b = RT/F \ln K \quad (3)$$

The values for **1b** and **2b** are 2.9×10^9 (ΔG=−53 kJ mol^{-1}) and 1.9×10^9 (ΔG=−52 kJ mol^{-1}), respectively, indicating that the mixed valence complexes are considerably stabilized. A dinuclear metal(II, II) complex must be more easily oxidized than a metal(II, III)

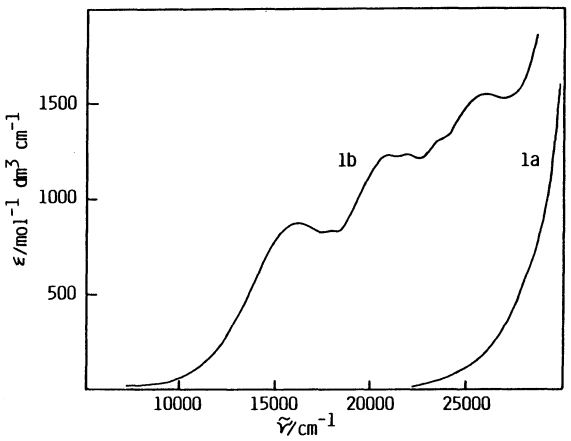

Fig. 4. Electronic spectra of $[Mn_2(L\text{-py})(CH_3COO)_2]$-$ClO_4\cdot0.5H_2O$ (**1a**) and $[Mn_2(L\text{-py})(CH_3COO)_2]$-$(ClO_4)_2\cdot H_2O$ (**1b**) in acetonitrile.

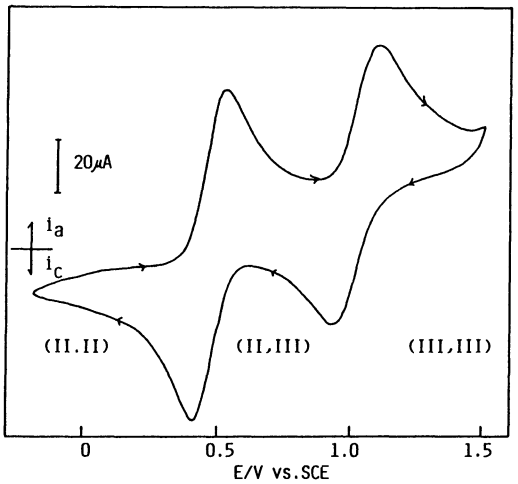

Fig. 5. Cyclic voltammogram of $[Mn_2(L\text{-py})$-$(CH_3COO)_2](ClO_4)_2\cdot H_2O$ (**1b**) in 0.1 mol dm^{-3} tetrabutylammonium perchlorate in acetonitrile at a glassy carbon electrode at a scan rate of 100 mV s^{-1}.

Table 6. Cyclic Voltammetric Data of the Mixed Valence Complexes

	Complex	$E_{1/2}{}^{a)}$ (E/V vs. SCE)	$E_{1/2}{}^{b)}$	$\Delta E^{a)}$ (ΔE/V)	$\Delta E^{b)}$	$R^{a)}$ ($i_{pa}{}^{d)}/i_{pc}{}^{e)}$)	$R^{b)}$	$K_c{}^{c)}$
1b	$[Mn_2(L\text{-py})(CH_3COO)_2](ClO_4)_2\cdot H_2O$	+0.47	+1.02	0.12	0.17	1.0	0.84	2.9×10^9
2b	$[Mn_2(L\text{-py})(C_6H_5COO)_2](ClO_4)_2\cdot H_2O$	+0.53	+1.07	0.10	0.12	1.0	0.84	1.9×10^9

(Experimental conditions: cf. Fig. 4) a) For Mn(II, III)/Mn(II, II) redox couple. b) For Mn(III, III)/Mn(II, III) redox couple. c) comproportionation constant at 20 °C. d) Anodic peak current. e) Cathodic peak current.

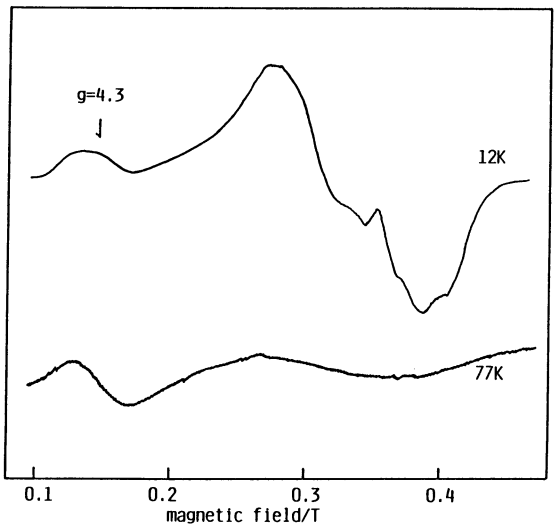

Fig. 6. ESR spectra of $[Mn_2(L\text{-py})(CH_3COO)_2](ClO_4)_2 \cdot H_2O$ (**1b**) in acetonitrile at 12 and 77 K. Spectral conditions: microwave power, 1 mW at 12 K and 2 mW at 77 K; microwave frequency, 9.036 GHz at 12 K and 9.041 GHz at 77 K; modulation amplitude, 0.25 mT at 12 K and 0.32 mT at 77 K at 100 kHz; receiver gain, 6.5×100 at 12 K and 3×1000 at 77 K.

one from electrostatic point of view. The electrostatic effect seems to be important, but a steric requirement of dinucleating ligand L-py and two bridging carboxylate ions may also play an important role. Actually, the reaction of an equimolar mixture of Fe^{3+} and Mn^{2+} ions with L-py and carboxylate ions afforded a dinuclear heterometal (II, III) complex $[FeMn(L\text{-py})(RCOO)_2]^{2+}$ with a slight contamination of homometal dinuclear complexes.[28] Thus, the present ligand system provides favorable coordination sites to M^{2+} and M^{3+} ions to form a mixed valence complex in the trapped valence state.

ESR Spectra. The ESR spectra of **1b** in acetonitrile were measured at 12 and 77 K. The spectrum at 12 K shows several resonances (Fig. 6). However, the signals almost disappear at 77K except for a signal at g=4.3. The g=4.3 signal may be ascribed to a distorted octahedral mononuclear manganese(II) complex with D and $E<0.1$ cm^{-1}, and $E/D \approx 1/3$[18] which is present as impurity formed by slight decomposition of the dinuclear complex. Such a temperature dependence of the signals suggests that the signals arise from the spin ground state of S=1/2. Mabad et al.[6] reported that the ESR of antiferromagnetically coupled dinuclear mixed valence manganese(II, III) complex shows a 16-hyperfine line ESR spectrum. As can be seen in Fig. 6, however, the present complexes show only broad signals.[29]

Finantial support from Ministry of Education, Science and Culture Grant-in-Aid for Scientific Research (No. 61540443) is gratefully acknowledged.

References

1) G. L. Lawrence and D. T. Sawyer, *Coord. Chem. Rev.*, **27**, 173 (1978).
2) K. Sauer, *Acc. Chem. Rev.*, **13**, 249 (1980).
3) T. Wydrzynski and K. Sauer, *Biochim. Biophys. Acta*, **589**, 56 (1980).
4) J. A. Kirby, D. B. Goodin, T. Wydrzynski, A. S. Robertson, and M. P. Klein, *J. Am. Chem. Soc.*, **103**, 5537 (1981).
5) H. Okawa, A. Honda, M. Nakamura, and S. Kida, *J. Chem. Soc., Dalton Trans.*, **1985**, 59.
6) B. Mabad, J. P. Tuchagues, Y. T. Hwang, and D. N. Hendrickson, *J. Am. Chem. Soc.*, **107**, 2801 (1985).
7) M. Suzuki, S. Murata, A. Uehara, and S. Kida, *Chem. Lett.*, **1987**, 281.
8) M. Suzuki, H. Kanatomi, and I. Murase, *Chem. Lett.*, **1981**, 1745.
9) C. P. Prabhakaran and C. C. Patel, *J. Inorg. Nucl. Chem.*, **30**, 867 (1968).
10) R. Blecher and T. S. West, *Anal. Chim. Acta*, **6**, 322 (1952).
11) E. B. Sandell, "Determination of Traces of Metals," 3rd ed, Interscience Publisher, New York (1959), p. 606.
12) "International Tables of X-Ray Crystallography," Kynoch Press, Birmingham (1974), Vol. 4.
13) T. Sakurai and K. Kobayashi, *Rikagaku Kenkyusho Hokoku*, **55**, 69 (1979).
14) P. Main, S. E. Hull, L. Lessinger, G. Germain, J. P. Declercq, and M. M. Woolfson, MULTAN 78, A System of Computor Programs for the automatic Solution of Crystal Structures from X-Ray Diffraction Data, University of York (1978).
15) C. K. Johnson, Report NO. ORNL3794, Oak Ridge National Laboratory, Oak Ridge, Tennessee (1965).
16) M. Mikuriya, N. Torihara, H. Okawa, and S. Kida, *Bull. Chem. Soc. Jpn.*, **54**, 1063 (1981) and references therein.
17) J. B. Vincent, K. Folting, J. C. Huffmann, and G. Christou, *Inorg. Chem.*, **25**, 996 (1986) and references therein.
18) B. Mabad, P. Cassoux, J. P. Tuchagues, and D. N. Hendrickson, *Inorg. Chem.*, **25**, 1420 (1986) and references therein.
19) a) K. Wieghardt, U. Bossek, D. Ventur, and J. Weiss, *J. Chem. Soc., Chemm. Commun.*, **1985**, 347; b) J. E. Sheats, R. S. Czernuszewicz, G. C. Dismukes, A. L. Rheingold, V. Petrouleas, J. Stubbe, W. H. Armstrong, R. H. Beer, and S. J. Lippard, *J. Am. Chem. Soc.*, **109**, 1435 (1987).
20) a) W. H. Armstrong, A. Spool, G. C. Papaefthymiou, R. B. Frankel, and S. J. Lippard, *J. Am. Chem. Soc.*, **106**, 3653 (1984) and references therein; b) K. Wieghardt, I. Tolksdorf, and W. Herrmann, *Inorg. Chem.*, **24**, 1230 (1985).
21) W. H. Armstrong and S. J. Lippard, *J. Am. Chem. Soc.*, **106**, 4632 (1984).
22) B. P. Murch, F. C. Bradley, and L. Que, Jr., *J. Am. Chem. Soc.*, **108**, 5027 (1986).
23) G. B. Deacon and R. J. Phillips, *Coord. Chem. Rev.*, **23**, 227 (1980).
24) M. Suzuki, A. Uehara, H. Oshio, K. Endo, M. Yanaga, S. Kida, and K. Saito, *Bull. Chem. Soc. Jpn.*, **60**, 3547 (1987).
25) a)J. I. Bullock, M. M. Patele, and J. E. Salmon, *J. Inorg. Nucl. Chem.*, **31**, 415 (1969); b) K. Yamaguchi and D. T. Sawyer, *Inorg. Chem.*, **24**, 971 (1985).

26) a) E. W. Aniscough, A. M. Brodie, J. E. Plowman, K. L. Brown, A. W. Addison, and A. R. Gainsford, *Inorg. Chem.*, **19**, 3655 (1980); b) J. W. Pyrz, A. L. Roe, L. J. Stern, and L. Que, Jr., *J. Am. Chem. Soc.*, **107**, 614 (1985).

27) M. Suzuki, A. Uehara, and K. Endo, *Inorg. Chim. Acta*, **123**, L9 (1986).

28) M. Suzuki, S. Murata, and A. Uehara, unpublished results.

29) Very recently, Diril et al. reported the crystal structure and ESR spectrum of **1b**. They observed a hyperfine structure (29 Mn hyperfine lines) at $g=2$ at 7.5 K. H. Diril, H. R. Chang, X. Zhang, S. K. Larsen, J. A. Potenza, C. G. Pierpont, H. J. Schugar, S. S. Isied, and D. N. Hendrickson, *J. Am. Chem. Soc.*, **109**, 6207 (1987).